The Determination of Kinematic Properties of a Wind Field Using Doppler Radar[1]

K. A. BROWNING[2]

Air Force Cambridge Research Laboratories, Sudbury, Mass.

AND R. WEXLER

Allied Research Associates, Inc., Concord, Mass.

(Manuscript received 27 July, in revised form 2 November 1967)

ABSTRACT

A technique is proposed for the measurement of kinematic properties of a wind field in situations of widespread precipitation, using a single Doppler radar to sense the motion of the precipitation particles. The technique is an extension of ideas put forward by Probert-Jones, Lhermitte, Atlas, Caton and Harrold, and is based upon the Velocity-Azimuth Display (VAD) obtained by scanning the radar beam about a vertical axis at a fixed elevation angle. Harmonic analysis of the VAD permits divergence to be obtained from the magnitude of the "zeroth" harmonic, wind speed and direction to be obtained from the amplitude and phase of the first harmonic, and resultant deformation and the axis of dilatation to be obtained from the amplitude and phase of the second harmonic. Although limitations to the accuracy of this technique are imposed by inhomogeneities in the horizontal distribution of precipitation fall speed and, in the presence of strong vertical wind shear, by elevation angle errors and reflectivity inhomogeneities, the errors resulting from these effects can be made acceptably small by scanning at appropriate elevation angles and ranges. An optimum scanning procedure is suggested. A short case study is also presented to support the view that meaningful estimates of mesoscale divergence and deformation can be obtained using this technique.

1. Introduction

Pulsed Doppler radar measures the line-of-sight velocity of targets within the pulse volume. When such a radar is used to observe precipitation in the free atmosphere, it detects a spread of velocities within each pulse volume. As is well known, the shape of the Doppler spectrum is influenced by a number of factors, such as wind shear and turbulence, and the intrinsic fall speed spectrum of the precipitation. The present paper, however, is not concerned so much with the shape of the Doppler spectrum as with the interpretation of the *mean* Doppler velocity, or spectrum first moment, observed at different orientations of the radar beam. As will become clear, measurements of the mean Doppler velocity within widespread precipitation can be most valuable for studying the wind field.

The use of pulsed Doppler radar to measure horizontal winds was first suggested by Probert-Jones (1960). Lhermitte and Atlas (1961) described in detail how such a radar could be used in situations of widespread precipitation to determine the wind speed and direction, and the precipitation fall speed, at different altitudes. They proposed a scanning mode in which the radar beam is directed at a constant elevation and is rotated about a vertical axis with the range gate set at a succession of altitudes of interest. As the beam rotates, the radar provides an output of the radial velocity of the precipitation particles vs azimuth; this is the so-called Velocity-Azimuth Display, or VAD. Lhermitte and Atlas showed that, provided the fields of wind and precipitation fall speed are horizontally homogeneous, the mean radial velocity is a sine function of azimuth angle. The amplitude and phase of this sine curve are measures of the speed and direction of the wind at the sampled altitude, and the displacement of the entire sine curve from the zero of velocity is a measure of the precipitation fall speed.

Caton (1963) extended Lhermitte and Atlas' ideas by pointing out that a convergent wind field produces a net radial velocity toward the radar, thereby affecting the VAD in a similar way to the mean precipitation fall speed. By scanning in the vertical between successive VAD cycles, Caton obtained independent estimates of the precipitation fall speed and was therefore able to infer the magnitude of the divergence. Caton did not, however, consider the errors introduced by horizontal inhomogeneities in fall speed. As Atlas (1964) and Lhermitte (1966) have emphasized, these errors can in some circumstances altogether invalidate the estimates of divergence.

[1] A shortened version of this paper appears in the *Proc. Twelfth Weather Radar Conf.*, Boston, Amer. Meteor. Soc., 1966.

[2] Present affiliation: Meteorological Office Research Unit, Royal Radar Establishment, Malvern, England.

The purpose of the present paper is to provide a general analysis of the VAD, valid for situations in which neither the field of wind velocity nor the field of precipitation fall speed is horizontally uniform. It is demonstrated that, provided certain precautions are observed to minimize the effects of fall speed inhomogeneities and vertical wind shear, the deviations of the mean radial Doppler velocity from a perfect sine curve constitute a reliable measure of several of the horizontal derivatives of wind velocity. A method is presented whereby not only divergence, but also the resultant deformation and the orientation of the axis of dilatation can be estimated simply from the VAD. The same method also provides for optimum accuracy in estimating the mean wind speed and direction.

2. Relationship of properties of a wind field to the VAD

Consider a Cartesian coordinate system with x positive toward the east, y positive toward the north, and z positive downward. Consider a ground-based Doppler radar located directly below the origin of the coordinate system; its beam is directed at elevation angle α and is rotating about a vertical axis with the range gate set at slant range R (horizontal range r) so as to scan a horizontal circle centered at the origin. Assume that the radar receives a return around the entire scanned circle from precipitation of fall speed V_f traveling with the wind at horizontal speed V_h and direction θ to the x axis (Fig. 1). The azimuth variation of the mean radial velocity sensed by the radar is then given by

$$\begin{aligned} V_R(\beta) &= -V_h(\beta)\cos(\beta-\theta)\cos\alpha + V_f(\beta)\sin\alpha \\ &= -V_x(\beta)\cos\beta\cos\alpha - V_y(\beta)\sin\beta\cos\alpha \\ &\quad + V_f(\beta)\sin\alpha, \quad (1) \end{aligned}$$

where V_R conventionally is positive toward the radar and V_f is positive downwards. The radar display of V_R as a function of β is the Velocity-Azimuth Display (VAD). The velocity components V_x and V_y may be

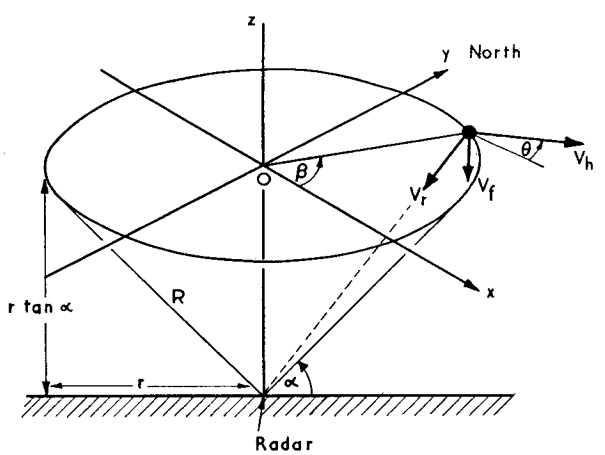

FIG. 1. Geometry of radar scan.

expressed in terms of their value at the center of the scanned circle (subscript 0) and mean linear velocity terms as follows:

$$V_x = V_{x0} + \overline{\frac{\partial V_x}{\partial x}}x + \overline{\frac{\partial V_x}{\partial y}}y,$$

$$V_y = V_{y0} + \overline{\frac{\partial V_y}{\partial x}}x + \overline{\frac{\partial V_y}{\partial y}}y.$$

Introducing these expressions into Eq. (1), with $x=r\cos\beta$ and $y=r\sin\beta$, and assuming for the present that the fall speed is horizontally homogeneous and equal to V_{f0}, gives

$$\begin{aligned} V_R(\beta) &= -\tfrac{1}{2}r\cos\alpha\left(\overline{\frac{\partial V_x}{\partial x}} + \overline{\frac{\partial V_y}{\partial y}}\right) + V_{f0}\sin\alpha \\ &\quad - V_{x0}\cos\alpha\cos\beta - V_{y0}\cos\alpha\sin\beta \\ &\quad - \tfrac{1}{2}r\cos\alpha\left(\overline{\frac{\partial V_x}{\partial x}} - \overline{\frac{\partial V_y}{\partial y}}\right)\cos 2\beta \\ &\quad - \tfrac{1}{2}r\cos\alpha\left(\overline{\frac{\partial V_x}{\partial y}} + \overline{\frac{\partial V_y}{\partial x}}\right)\sin 2\beta. \quad (2) \end{aligned}$$

Eq. (2) can be decomposed into a Fourier series of form

$$V_R = \tfrac{1}{2}a_0 + \sum_{n=1}^{\infty}(a_n\cos n\beta + b_n\sin n\beta).$$

The non-zero Fourier coefficients are given by:

$$a_0 = -r\cos\alpha\left(\overline{\overline{\frac{\partial V_x}{\partial x}}} + \overline{\overline{\frac{\partial V_y}{\partial y}}}\right) + 2V_{f0}\sin\alpha,$$

$$a_1 = -V_{x0}\cos\alpha,$$

$$b_1 = -V_{y0}\cos\alpha,$$

$$a_2 = -\tfrac{1}{2}r\cos\alpha\left(\overline{\overline{\frac{\partial V_x}{\partial x}}} - \overline{\overline{\frac{\partial V_y}{\partial y}}}\right),$$

$$b_2 = -\tfrac{1}{2}r\cos\alpha\left(\overline{\overline{\frac{\partial V_x}{\partial y}}} + \overline{\overline{\frac{\partial V_y}{\partial x}}}\right),$$

where the double bars indicate integral means of the derivatives. The terms

$$\left(\overline{\overline{\frac{\partial V_x}{\partial x}}} + \overline{\overline{\frac{\partial V_y}{\partial y}}}\right), \quad \left(\overline{\overline{\frac{\partial V_x}{\partial x}}} - \overline{\overline{\frac{\partial V_y}{\partial y}}}\right) \quad \text{and} \quad \left(\overline{\overline{\frac{\partial V_x}{\partial y}}} + \overline{\overline{\frac{\partial V_y}{\partial x}}}\right)$$

correspond, respectively, to the two-dimensional horizontal divergence, stretching deformation, and shearing deformation, Thus, the kinematic properties of the wind

field can be obtained from the Fourier coefficients as follows:

Divergence:

$$\mathrm{div}\mathbf{V}_h = -\frac{a_0}{r\cos\alpha} + \frac{2V_{f0}}{r}\tan\alpha \tag{3}$$

Wind speed:

$$V_h = -(a_1^2+b_1^2)^{\frac{1}{2}}/\cos\alpha \tag{4}$$

Wind direction:

$$\left.\begin{aligned}\theta &= \frac{\pi}{2} - \tan^{-1}\frac{a_1}{b_1}, \text{ when } b_1 \text{ is negative}\\ &= \frac{3\pi}{2} - \tan^{-1}\frac{a_1}{b_1}, \text{ when } b_1 \text{ is positive}\end{aligned}\right\} \tag{5}$$

Resultant deformation:

$$\mathrm{def}_r\mathbf{V}_h = -2(a_2^2+b_2^2)^{\frac{1}{2}}/r\cos\alpha \tag{6}$$

Orientation of the axis of dilatation:

$$\left.\begin{aligned}\gamma &= \frac{\pi}{4} - \tfrac{1}{2}\tan^{-1}\frac{a_2}{b_2}, \text{ when } b_2 \text{ is negative}\\ &= \tfrac{3}{4}\pi - \tfrac{1}{2}\tan^{-1}\frac{a_2}{b_2}, \text{ when } b_2 \text{ is positive}\end{aligned}\right\} \tag{7}$$

A graphical illustration of the relationship of these quantities to the VAD is shown in Fig. 2. Note that θ and γ are each measured counterclockwise with respect to the x axis; the conventionally-defined wind direction is given by $\left(\frac{3\pi}{2}-\theta\right)$. Also note that the resultant deformation, $\mathrm{def}_r\mathbf{V}_h$, reduces to the stretching deformation, $\mathrm{def}\mathbf{V}_h$, when $\gamma=0$ (i.e., $b_2=0$) and to the shearing deformation, $\mathrm{def}'\mathbf{V}_h$, when $\gamma=\pi/4$ (i.e., $a_2=0$). Individual values of $\overline{\overline{\partial V_x/\partial x}}$ and $\overline{\overline{\partial V_y/\partial y}}$ may be computed from half the sum and difference, respectively, of $\mathrm{div}\mathbf{V}_h$ and $\mathrm{def}\mathbf{V}_h$.

If V_R is measured at 10° intervals of azimuth, the Fourier coefficients can be computed in the normal way from

$$a_0 = \frac{1}{18}\sum_{i=1}^{36} V_{R_i},$$

$$a_n = \frac{1}{18}\sum_{i=1}^{36} V_{R_i}\cos n\beta_i,$$

$$b_n = \frac{1}{18}\sum_{i=1}^{36} V_{R_i}\sin n\beta_i,$$

where $n=1$ or 2. It is sometimes of interest to compute the stretching and shearing deformations within a coordinate system in which the x axis is drawn parallel to the wind direction at the appropriate altitude. This is done most easily by recomputing coefficients a_2' and b_2' as follows:

$$a_2' = a_2\cos 2\theta + b_2\sin 2\theta,$$

$$b_2' = b_2\cos 2\theta - a_2\sin 2\theta.$$

By varying α and/or r between successive VAD scans it is possible to measure the quantities in Eqs. (3)–(7) as a function of altitude. There is, however, an upper limit to α above which fall speed begins to contaminate the results excessively (see Section 3). There is also an upper limit to r set by the radar pulse repetition frequency, by the need for most of the scanned circle to be filled with detectable precipitation, and by the errors to be discussed later in Section. 4. These limitations combine to restrict the maximum altitude to which this technique can be applied. The lower limits of α and r, set by the radar horizon and the receiver recovery time, respectively, are usually such as to permit very low altitudes to be sampled. Since the coefficients of the zeroth and second harmonics, from which the divergence and deformation are obtained, are generally small compared with that of the fundamental, their accuracy of measurement is optimized by making r as large as possible within the limitations noted above. In practice, r is of the order of 10 km for which the velocity differences associated with the divergence and deformation terms, $r\,\mathrm{div}\mathbf{V}_h$ and $r\,\mathrm{def}_r\mathbf{V}_h$, turn out to be of the order of 1 m sec^{-1}. Clearly, therefore, it is necessary to keep errors in V_R smaller than 1 m sec^{-1}.

Some of the major sources of error in the interpretation of the VAD have been discussed by Harrold (1966). In particular, he has considered the effect of random and systematic errors in the measurement of V_R and also the effect of constant backlash errors in the measurement of α. He suggests that when $\alpha \leqslant 15°$, these errors together are unlikely to lead to errors in the estimated divergence exceeding 5×10^{-5} sec^{-1} at a height of 2 km or twice this value at 1 km. A possible source of error not considered by Harrold is the time variation of the wind field during the period of a single azimuth rotation. In general, however, a rotation rate of 1 rpm is thought to be fast enough to render such errors quite small. This is because in 1 min the pattern of airflow is unlikely to travel much further than 1 km, which is an order of magnitude less than the diameter of the circle over which the kinematic properties are normally averaged.

Other errors, not considered by Harrold, are produced by inhomogeneities in the horizontal distribution of precipitation fall speed and also, in the presence of strong vertical wind shear, by a slightly nonvertical axis of rotation or by reflectivity inhomogeneities. These additional sources of error are now considered in some detail because they imply limitations as to the way in which the data should be acquired.

3. Limitations due to the effect of inhomogeneities in precipitation fall speed

So far it has been assumed for simplicity that the mean precipitation fall speed V_f is horizontally homogeneous over the area of the scanned circles. In general, however, this is not the case. Fluctuations of the mean (reflectivity weighted) fall speed are produced both by variations in vertical air velocity and by variations in the shape and width of the terminal fall speed spectrum of the precipitation particles. In widespread precipitation the vertical velocities are generally of the order of tens of cm sec^{-1}, although in the less stable situations, vertical velocities an order of magnitude greater may occur locally. Variations of the mean terminal fall speed of the particles, on the other hand, although usually less than 1 m sec^{-1} in snow, can be as great as 4 m sec^{-1}

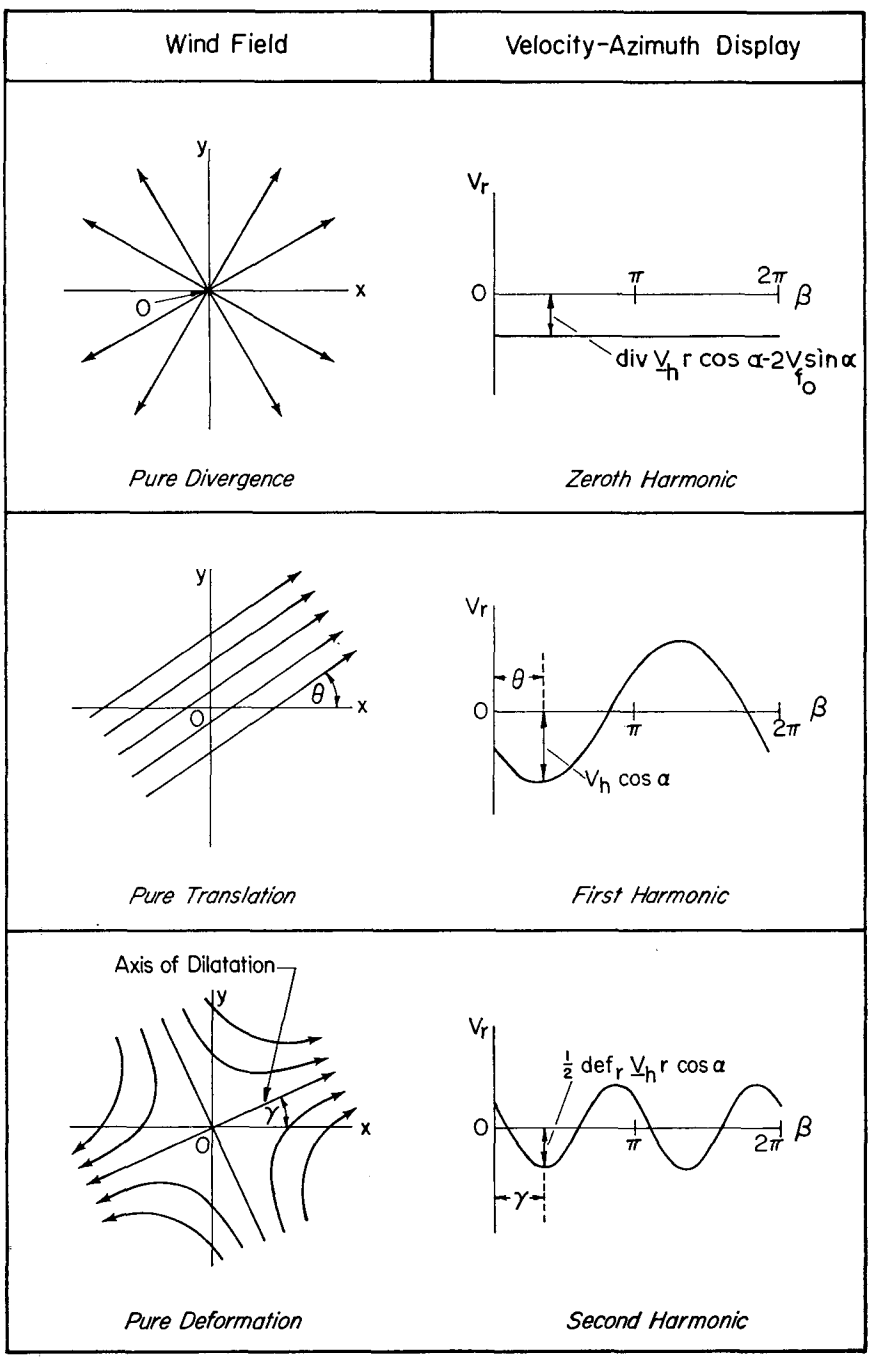

FIG. 2. Three simple windfields and the corresponding VAD's.

in rain. In extreme cases these effects may combine to produce fluctuations of up to 2 m sec^{-1} in snow and 6 m sec^{-1} in rain. Fortunately, however, the fluctuations are usually far smaller than this [as, for example, in the case study of Harrold (1966) in which the maximum fluctuations in rain were less than 1 m sec^{-1}].

In practice, the fall speed V_{f0} directly above the radar is measured by scanning vertically between successive VAD cycles. As suggested by Harrold time running means of V_{f0} are obtained in order to minimize the effect of unrepresentative vertical soundings of fall speed. The resulting values of V_{f0} are then assumed to be representative of the circles scanned in the VAD cycles. Although spatial variations of the fall speed along the direction of travel of the precipitation system may be inferred crudely from the temporal change of V_{f0} on the assumption that the pattern is translating over the radar in a steady state, no means are available for inferring accurately from a single Doppler radar changes in mean fall speed on either side of the radar. Therefore, it is essential that the contribution of the fall speed to the radial Doppler velocity V_R be kept as nearly as possible negligibly small. Now an error δV_f gives rise to an error δV_h in the inferred value of the horizontal wind given by $\delta V_f \tan\alpha$ so that, in order to keep δV_h smaller than 1 m sec^{-1} in the presence of the extreme fall speed variability mentioned above, it is necessary to keep $\alpha < 27°$ in snow and $\alpha < 9°$ in rain. In order to hold the fall speed contamination to a minimum, it is a good practice to keep α smaller than these values even in the more usual circumstances when the field of fall speed is more nearly homogeneous than has been assumed above.

4. Limitations due to the effect of vertical wind shear

In the presence of vertical wind shear, the radar may sense false horizontal derivatives of velocity owing to a failure to sense the winds within a perfectly horizontal plane. In situations of widespread precipitation, it is not uncommon for the vertical shear, $(\partial V_h/\partial z)$, to be as large as 10^{-2} sec^{-1} over height intervals of several hundred meters. Therefore, in order to keep the error δV_h smaller than 1 m sec^{-1}, when the radar beam is oriented parallel to the wind shear vector, it is necessary to ensure that the height error $\delta z < 100$ m. Now, errors in z may arise due to variations of elevation angle or to inhomogeneities in reflectivity distribution.

a. Variations of elevation angle during a single VAD scan. One of the advantages of the VAD technique for investigating the wind at any given level is that it entails the measurement of velocity components during the rotation of the antenna at a single elevation angle; comparisons of values measured at different elevation angles are avoided. What matters, therefore, is not so much the absolute accuracy with which α may be measured but, rather, how nearly constant α remains during a single 360° rotation of the antenna. Provided that the antenna is mounted on a solidly constructed pedestal and is enclosed within a radome to reduce the effect of strong surface winds, it should be possible to keep $\delta\alpha \leqslant 0.25°$ during a single rotation. Now, $z = r\tan\alpha$, so that $\delta z = r\,(\sec^2\alpha)\delta\alpha$. Over the entire permissible range of α, from 0°–27°, $\sec\alpha$ is fairly close to unity, and so, for $\delta z < 100$ m, it is necessary to keep $r \leqslant 23$ km.

b. Inhomogeneities in reflectivity distribution. As already mentioned, a spread of velocities is detected within each pulse volume as a result of wind shear and turbulence (and, to a lesser extent, differential particle fall speeds when operating at the higher elevation angles). The mean radial velocity V_R is, of course, weighted in favor of the velocities associated with the highest reflectivity. If there is a homogeneous spatial distribution of reflectivity and a linear vertical wind shear within the pulse volume, the measured mean velocity will be a good representation of the velocity at the center of the pulse volume. If, on the other hand, there are inhomogeneities in the distribution of reflectivity within the pulse volume, the measured mean velocity may be weighted in favor of a velocity characteristic of a level other than that at the center of the pulse volume. In the presence of vertical wind shear, variations in the height of this level around the scanned circle will lead to the detection of spurious variations in V_h.

Errors of this kind that arise because of the finite pulse length are easily shown to be small for pulse lengths of the order of 1 μsec or less. The effect of the finite beam width can be calculated on the assumption that the antenna radiation pattern $I(\phi)$ is Gaussian. Following Donaldson (1965), the antenna pattern function may be described by

$$I^2 = I_0^2 \exp[-\ln 4(z/r\phi_0)^2], \tag{8}$$

where I_0 is the value of I along the beam axis at $\phi = 0$, $2\phi_0$ is the angular beamwidth to half power points, and z is height above the beam axis at range r. Therefore, in the presence of an exponential vertical distribution of reflectivity proportional to e^{kz}, the peak power will be returned from a level above the beam axis corresponding to a height error of

$$\delta z = \frac{k\phi_0^2 r^2}{\ln 4}. \tag{9}$$

In order to infer a limiting value for this error, it is necessary to consider the largest vertical reflectivity gradient likely to be encountered in widespread precipitation. Of course, the largest gradients, about 6 db within 100 m, occur at the level of a radar bright band, where falling snowflakes abruptly increase in reflectivity as they begin to melt [see, for example, Fig. 40 of Atlas (1964)]. Where the bright band is horizontal this gives rise to a height error that is constant around the scanned circle and which is therefore relatively un-

important. Outside the bright band in widespread precipitation, the vertical gradient of reflectivity seldom exceeds 2 db per 100 m ($k=4.6\times10^{-5}$ cm^{-1}) and usually is much less. Eq. (9) shows that such a gradient will produce a height error δz of $2.6\times10^{-9}\,r^2$ (cgs units) in the case of a radar with a beam width of 1°. The maximum permissible height error of 100 m is therefore not exceeded unless the horizontal range is greater than 20 km. This is comparable with the range of 23 km that was estimated to be the maximum range permitted by the elevation angle errors.

5. An optimum scanning procedure

The optimum range for minimizing errors in the VAD technique can be obtained from Fig. 3. Three lines are plotted in this figure; the one at 20 km range is an upper range limit set by errors due to vertical wind

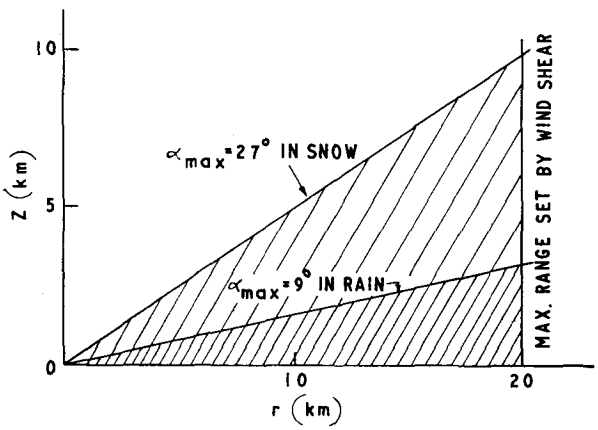

FIG. 3 Permissible scanning ranges and heights for optimum accuracy in widespread snow and rain, calculated for a radar with a half-power beam width of 1°; for a 2° beam all ranges should be halved.

shear (Section 4), and the other two are upper limits to the elevation angles in snow and rain, set by errors due to fall speed inhomogeneities (Section 3). Of course, Fig. 3 should not be interpreted too rigidly. If, for example, there is reason to believe that the field of precipitation fall speed is relatively homogeneous, then the elevation angle restrictions can be relaxed accordingly. Choice of operating range within the above limitations is a compromise between three considerations:

1) Higher altitudes can be observed only at longer ranges.

2) The accuracy of estimates of divergence and deformation is enhanced by making the coefficients of the zeroth and second harmonics as large as possible, and this is achieved by working at longer ranges.

3) A large proportion of the scanned circle must be filled with detectable precipitation, and this is most likely to occur at the shorter ranges.

Caton (1963) and Harrold (1966) have measured wind velocities and divergence at various altitudes with the VAD technique by range-gating at a number of ranges, with α kept constant at 15° or 30°. Although this procedure has the advantage of simplicity and of permitting many ranges to be observed simultaneously, it has the disadvantage of always operating close to, and sometimes above, the upper limit of permissible α; moreover, the areas viewed at the lower altitudes are small and liable to be unrepresentative. Hence, in order to optimize both α and r, and also to ensure that the properties of the wind field are averaged over more or less the same horizontal area at all altitudes, it is preferable to obtain VAD's at a sequence of elevation angles. This leads to a VAD scanning sequence called SEVAD (Stepped Elevation Velocity-Azimuth Displays).

6. An actual data collection procedure

Although errors due to the factors discussed in Sections 3 and 4 may, even with an optimized data acquisition scheme, sometimes be as great as 1 m sec^{-1}, it is expected that in most cases the errors will be far smaller than this. Thus, it is desirable to have data acquisition and processing equipment that will permit the mean value of V_R to be measured and displayed accurately to within, say, 0.2 m sec^{-1}. Particular care must be taken to avoid systematic errors since, for example, with $r=20$ km, a systematic error of only 0.1 m sec^{-1} would lead to an error of about 10^{-5} sec^{-1} in the estimated diverence. A set-up that came close to attaining this kind of accuracy was first put into operation on 13 December 1965 using the Porcupine Doppler radar at AFCRL, Bedford, Mass.

The Porcupine radar is a pulse Doppler operating on a wavelength λ of 5.42 cm. Its 6-m diameter antenna provides a pencil beam 1° wide between half power points. On 13 December it was operated at a peak power of 20 kW, with a pulse repetition frequency (PRF) of 3300 sec^{-1} and a pulse length of 2 μsec. The antenna was rotated continuously about a vertical axis at 1.3 rpm, with its 0.5-μsec wide movable range gate set at $R=18$ km. After each rotation, the beam was elevated by 2°, starting with $\alpha=2°$ and ending with $\alpha=20°$. The properties of the wind field were therefore obtained as averages over horizontal areas of between 900 and 1000 km^2. In order to enhance the accuracy of the harmonic analysis of the VAD's, velocity data were obtained for a complete 360° rotation at each elevation step. At a rotation rate of 1.3 rpm, the antenna rotated through almost 20° in the time taken for it to reach a new elevation step; thus, it was necessary to commence each new VAD scan 380° after the beginning of the previous one. Upon completion of the final scan, at 20° elevation, the beam was pointed vertically and the gate scanned in range to obtain a vertical sounding of V_{f0}. The entire SEVAD cycle, taking 8 min to complete, was controlled by means of an automatic program.

Throughout the scanning cycles, the phase detected

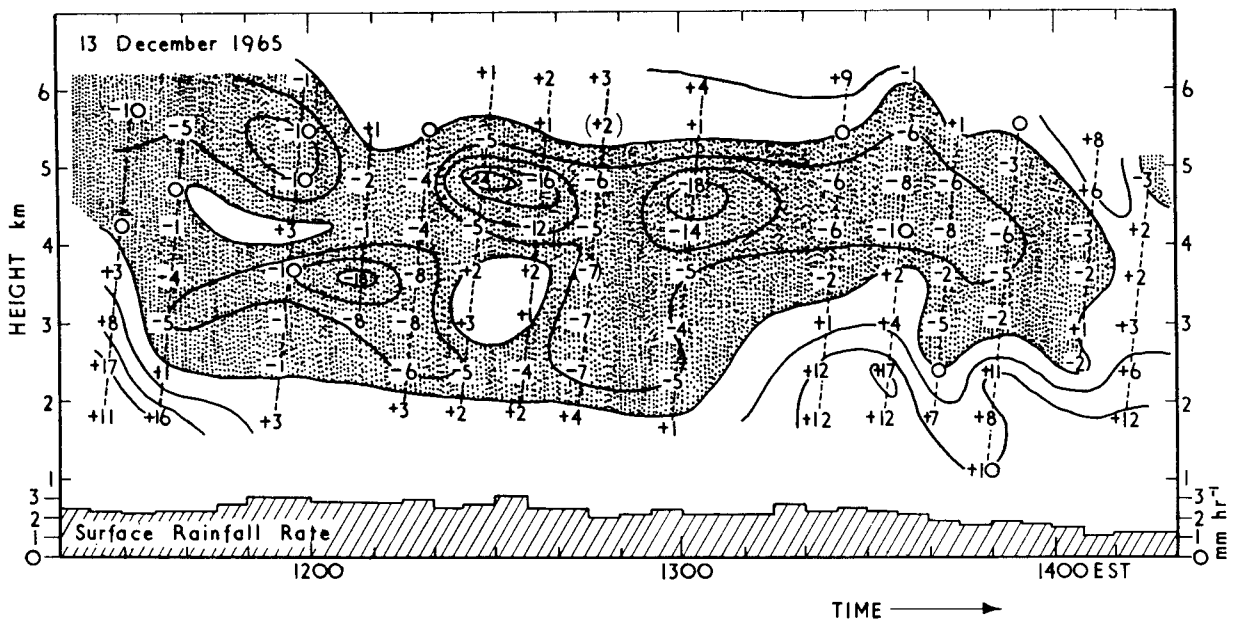

FIG. 4. Time-height pattern of divergence in units of 10^{-5} sec^{-1}. Surface rainfall rate is shown along the abscissa.

bi-polar video was recorded on magnetic tape, together with digital azimuth and elevation information and supplementary voice comments. Subsequently, the phase detected bi-polar video was fed into an audio frequency analyzer. The outputs from the 100 filters of the frequency analyzer were scanned sequentially by a commutator at the rate of 30 complete scans per second and after each revolution of the commutator a synchronizing signal was generated which permitted the horizontal deflection of the spot on an oscilloscope display to be directly proportional to Doppler velocity. The filter output was then used to intensity modulate the scope at the position being sampled at any given instant. The oscilloscope display was photographed using a 35-mm strip film travelling continuously at 3 mm sec^{-1} in a vertical direction.

Two sources of error in the measurement of V_R must be considered. The first arises from fundamental limitations to the accuracy due to the incoherent nature of the backscatter from the precipitation particles, and the second arises from the nature of the radar and frequency analyzer. With regard to the former, Cox and Groginsky (1966) have derived an expression for the variance $\sigma_{V_R}^2$ of the estimate of the mean Doppler velocity obtained while the beam rotates through a single beamwidth. They show that $\sigma_{V_R}^2=\lambda^2 B/(8T_S\theta)$, where B is the signal bandwidth, T_S the time taken for one complete azimuth rotation and θ the antenna beamwidth. For the parameters appropriate to this study, and for a bandwidth of 100 cps corresponding to a velocity spread of 2.7 m sec^{-1}, $\sigma_{V_R}^2$ turns out to be 400 cm^2 sec^{-2}, i.e., a standard deviation of only 0.2 m sec^{-1}.

The frequency stability of the Porcupine Doppler radar is excellent and errors in the measured Doppler frequency shift f are unlikely to have exceeded 2 cps. The 100 filters comprising the frequency analyzer were calibrated frequently and were accurate to within 1 cps. The maximum error of 3 cps for individual filters corresponds to an error in V_R of under 0.1 m sec^{-1}, which is smaller than the standard deviation due to the statistical properties of the signal. Accurate measurement of the mean Doppler velocity was hindered, however, by the poor intensity modulation achieved by the photographic recording technique used in the present study; nevertheless, the random error of individual estimates of V_R was probably only about 0.2–0.4 m sec^{-1}.

7. An experimental test of the accuracy of measurements of divergence and deformation

The accuracy of the computed divergence and deformation depends rather sensitively upon the fall speed and reflectivity inhomogeneities around the scanned circles. Therefore, rather than attempting to determine the accuracy from a conventional error analysis, it had been decided instead to analyze the internal consistency of the pattern of these quantities using the data obtained with the Porcupine radar on 13 December 1965.

The radar was operated from 1120 until 1420 EST on 13 December during which time the surface pressure was falling steadily by between 1.0 and 1.7 mb hr^{-1} in association with an eastward-moving short-wave trough. Rain fell fairly steadily throughout the period, with 5-min intensities between 1 and 3 mm hr^{-1}. The melting level was at an altitude of 1800 m so that, with the range gate set at 18 km, the only VAD scans made within rain were those with $\alpha<6°$, which is within the limits specified in Fig. 3.

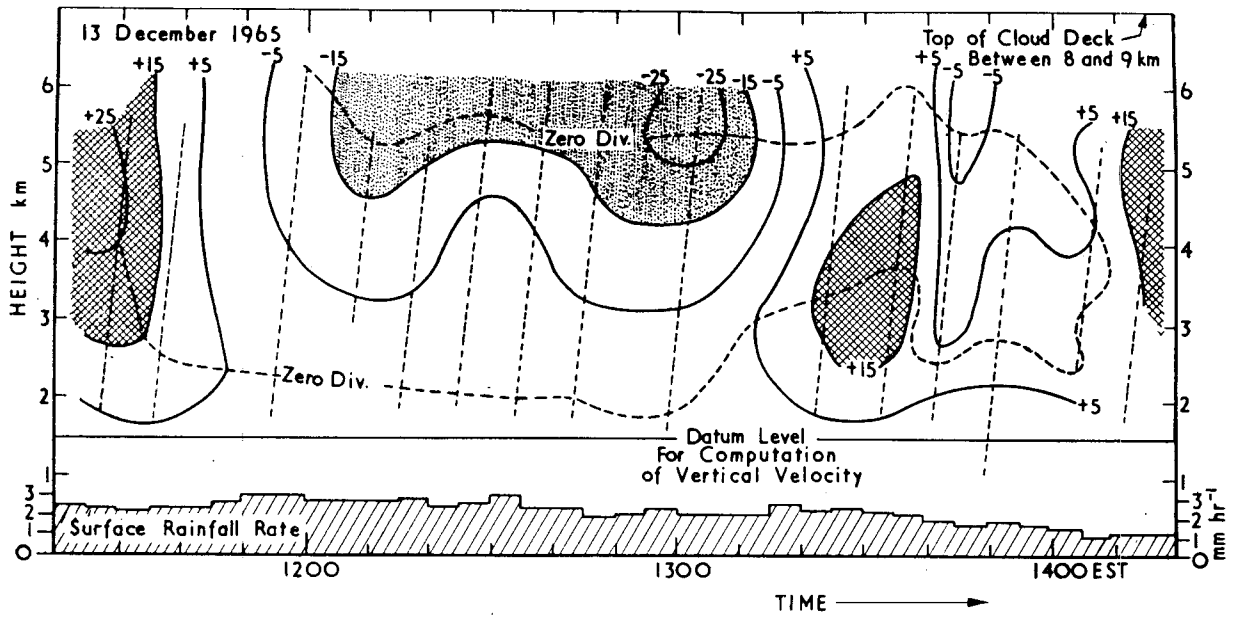

FIG. 5. Time-height pattern of vertical air velocity in cm sec^{-1} (positive downward). Surface rainfall rate is shown along the abscissa.

Fig. 4 shows the time-height pattern of divergence as computed from Eq. (3). Unfortunately, for technical reasons, the data below about 1.5 km were unusable on this occasion. Evidently convergence (negative D) was strongest at heights of 3–5 km; divergence was strongest below 2 km. The largest values were about $\pm 2\times 10^{-4}$ sec^{-1}, almost an order of magnitude smaller than the values observed by Harrold (1966) on somewhat smaller scales. The surface rainfall rate is plotted at the base of Fig. 4. Because of wind shear and the time for precipitation to descend, the surface rainfall rate was not closely related to the distribution of convergence directly over-

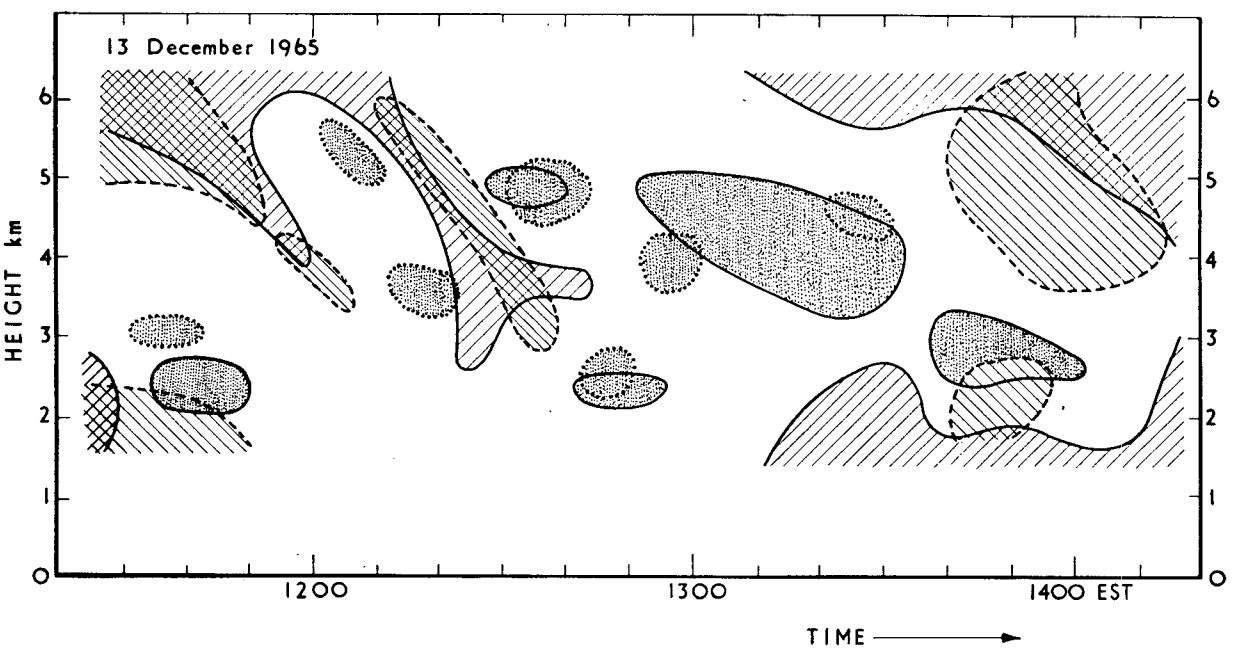

FIG. 6. Time-height patterns of $\overline{\overline{\partial V_x/\partial x}}$ and $\partial V_{x_0}/\partial t$, with the x direction along the direction of the wind. The solid contours represent the distribution of $\overline{\overline{\partial V_x/\partial x}}$, hatched areas denoting positive values greater than $+5\times 10^{-6}$ sec^{-1} and the stippled areas denoting negative values smaller than -5×10^{-5} sec^{-1}. The dashed and dotted contours represent the distribution of $\partial V_{x_0}/\partial t$, hatched areas denoting values smaller than -0.5 m sec^{-1} (10 min)$^{-1}$ and the stippled areas denoting values greater than $+0.5$ m sec^{-1} (10 min)$^{-1}$.

head; however, during the last hour there was a decrease of rainfall rate coincident with an overall decrease in convergence aloft.

Vertical integration of the pattern of divergence reveals an extensive region of gentle updraft between 1200 and 1310 EST, preceded and followed by widespread subsidence (Fig. 5). As pointed out by Harrold (1966), errors in vertical velocity accumulate with height and may become large at high levels. Moreover, distortion of the pattern of vertical velocity at high levels may have resulted from undetermined pockets of vertical velocity below 1.5 km. Although it is difficult to obtain reliable estimates of the errors involved, the coherency of the profiles of vertical velocity from one SEVAD cycle to the next lends confidence to the overall validity of the patterns in Figs. 4 and 5, especially before 1310 EST.

Finally, Fig. 6 has been prepared in order to shed light on the reliability of the estimates of deformation. The solid contours in Fig. 6 represent the distribution of $\overline{\overline{\partial V_x/\partial x}}$, with the x direction along the direction of the wind, as obtained from half the sum of the stretching deformation and the divergence. The dashed and dotted contours in Fig. 6 represent the distribution of $\partial V_{x_0}/\partial t$ averaged over 10-min periods, as obtained from time changes in the value of V_{x_0}. If the pattern of airflow had been in a steady state and translating across the Doppler radar at 17 m sec^{-1}, then the distributions of $\overline{\overline{\partial V_x/\partial x}}$ and $\partial V_{x0}/\partial t$ would be expected to show a similar pattern. Fig. 6 shows that the correspondence was, in fact, remarkably good before 1300 EST but that it deteriorated thereafter. This internal consistency provides good evidence of the reliability of the estimates of $\overline{\overline{\partial V_x/\partial x}}$, at least until 1300 EST; the poorer correspondence afterwards may have been due either to unsteadiness in the airflow pattern or to greater errors in the technique. The fact that the pattern of $\overline{\overline{\partial V_x/\partial x}}$ was obtained from the sum of the divergence and deformation patterns lends confidence to the validity of both of these patterns.

An alternative method of estimating the accuracy of this technique would have been to compare results obtained at different elevation angles with the range gate adjusted to fall at the same altitude.

8. Summary and conclusions

A straightforward technique has been proposed for the measurement of the kinematic properties of a wind field using a single Doppler radar in situations of widespread precipitation. Harmonic analysis of the conventional Velocity-Azimuth Display (VAD) permits divergence to be obtained from the magnitude of the "zeroth" harmonic, wind speed and direction to be obtained from the amplitude and phase of the fundamental, and resultant deformation and the orientation of the axis of dilatation to be obtained from the amplitude and phase of the second harmonic. The only linear property of motion that cannot be evaluated by this technique is vorticity; clearly, a single conventional Doppler radar cannot be expected to yield the latter from this kind of analysis, since it is not capable of measuring tangential velocities around the scanned circle.

The estimate of wind velocity obtained by this technique is more accurate than that obtained conventionally from the magnitudes of the maximum and minimum in the VAD because data are used from many more points around the scanned circle. Although limitations to the accuracy of measuring divergence and deformation are imposed by inhomogeneities in the horizontal distribution of precipitation fall speed and, in the presence of strong vertical wind shear, by elevation angle errors and reflectivity inhomogeneities, errors from these effects can be made acceptably small by scanning at appropriate elevation angles and ranges in accordance with Fig. 3. It should be emphasized, however, that the elevation angle restriction is quite severe in the presence of nonuniform rainfall or appreciable convection. A short case study of the kinematic properties of the airflow associated with an area of widespread rain has supported the view that meaningful estimates of divergence and deformation can be obtained using this technique.

Acknowledgments. The authors are grateful to Messrs. G. Armstrong, E. Duquette and C. Landry (AFCRL) and F. Compton (Raytheon Company) for their assistance in collecting and processing the radar data, and to Mr. D. Aiken (AFCRL) for running the harmonic analysis computer program.

REFERENCES

Atlas, D., 1964: Advances in radar meteorology. *Advances in Geophysics*, Vol. 10, New York, Academic Press, 317–478.

Caton, P. A. F., 1963: Wind measurement by Doppler radar. *Meteor. Mag.*, **92**, 213–222.

Cox, E. G., and H. L. Groginsky, 1966: An analysis of the estimates of wind parameters using the VAD technique. *Proc. Twelfth Weather Radar Conf.*, Boston, Amer. Meteor. Soc., 44–51.

Donaldson, R. J., Jr., 1965: Resolution of a radar antenna for distributed targets. *J. Appl. Meteor.*, **4**, 727–740.

Harrold, T. W., 1966: Measurement of horizontal convergence in precipitation using a Doppler radar. *Quart. J. Roy. Meteor. Soc.*, **92**, 31–40.

Lhermitte, R. M., 1966: Application of pulse Doppler radar technique to meteorology. *Bull. Amer. Meteor. Soc.*, **47**, 703–711.

——, and D. Atlas, 1961: Precipitation motion by pulse Doppler. *Proc. Ninth Weather Radar Conf.*, Boston, Amer. Meteor. Soc., 218–223.

Probert-Jones, J. R., 1960: Meteorological use of pulse Doppler radar. *Nature*, **186**, 271–273.